

# Semi-automated cell counting in phase contrast images of epithelial monolayers

Rachel Flight<sup>1</sup> rxf144@bham.ac.uk

Gabriel Landini<sup>2</sup> g.landini@bham.ac.uk

Iain Styles<sup>3</sup> i.b.styles@cs.bham.ac.uk

Richard Shelton<sup>2</sup> r.m.shelton@bham.ac.uk

Michael Milward<sup>2</sup> m.r.milward@bham.ac.uk

Paul Cooper<sup>2</sup> p.r.cooper@bham.ac.uk

<sup>1</sup> PSIBS DTC, University of Birmingham, UK

<sup>2</sup> School of Dentistry, University of Birmingham, UK

<sup>3</sup> School of Computer Science, University of Birmingham, UK

## Abstract

Non-destructive, quantitative evaluation of cell numbers in epithelial monolayers is necessary to monitor their proliferative rate in a single culture over a time period. Imaging using phase contrast microscopy is non-invasive and creates contrast in optically transparent cells; however intrinsic image artefacts mean that thresholding-based segmentation methods alone are insufficient to identify cells. The method described uses mathematical morphology to assign contrast to cells in a way that enables approximate segmentation by applying a threshold value. K-means clustering is subsequently applied to improve enumeration accuracy by removing segmentation artefacts. Cell numbers in images over multiple time-points may then be used to non-destructively generate growth curves. To validate this method we demonstrate a dose dependent relationship between H400 keratinocyte proliferation and concentration of foetal calf serum.

## 1 Introduction

Epithelial keratinocytes form stratified structures in regions of the body where their robust response to stress is essential, for example, in the masticatory mucosa. When the continuity of epithelial tissue is broken, keratinocytes respond by increasing proliferation and migrate into the wound to close it and prevent dehydration and infection [1]. Keratinocytes cultured *in vitro* form monolayers, which can be thought of as a simplified, 2D model of epithelium and are frequently used to study cell behaviour. The growth of such cultures in response to a stimulus may be assessed using cell counts obtained at multiple time-points.

The most widely-used method for determining cell number in cultures is by dissociating cells from their substrate, re-suspending and manually counting them on a haemocytometer using a microscope. The destructive nature of this technique means it is necessary to simultaneously maintain several cultures to generate growth curves. Small variations in the initial seeding densities of each culture or dilution upon re-suspension introduce error into the cell counts, therefore these are often performed at least in triplicate, which consumes both time and laboratory resources. Furthermore, operator variability contributes strongly to the count error [2].

Phase contrast (PC) microscopy creates contrast non-invasively in optically transparent objects using small changes in the phase of transmitted light so PC images of cell cultures

© 2014. The copyright of this document resides with its authors.

It may be distributed unchanged freely in print or electronic forms.

provide a potential approach for non-destructive cell counting. However, PC images are subject to intrinsic artefacts in the form of a ‘halo effect’: regions of high intensity pixels found at the edges of objects (Figure 1a). As a consequence, simple thresholding techniques are unsuccessful at distinguishing cells from background in PC images.

PC image analysis techniques frequently fall into two groups: textural analysis of entire images to distinguish between cell-populated and background regions, and high precision segmentation of individual cells. Methods in the first group are unable to provide information relating to individual cells and are not applicable at very low cell densities [3]. Conversely, methods in the second group are unsuitable for segmenting cells in dense images since they require time-consuming initialisation and high computational power [4]. Neither of these approaches is appropriate for both low and high density images of cell cultures, as is required to generate a comprehensive growth curve.

An alternative approach for locating cells in PC images involves correcting the halo artefact by using a mathematical model of PC optics to deconvolve images [5]. However this method is computationally expensive and therefore unsuitable for use on large images. A quicker, approximated form of deconvolution has been used to locate epithelial cells in scratch wound assays but to our knowledge has not been used to accurately count cells [6].

Lack of contrast in the related technique of brightfield microscopy makes it generally unsuitable for imaging unstained cells, but when the imaging plane is moved slightly above the focal plane, contrast increases such that cells become brighter than the background, albeit at the expense of subcellular detail. The opposite contrast is observed when the imaging plane moves below the focal plane, i.e. cells become darker. Dehlinger *et al.* located cells in a monolayer by subtraction of two such images acquired with the objective lens displaced by 15  $\mu\text{m}$  [7]. However, this relatively small distance is difficult to achieve consistently without costly automated imaging apparatus.

In this paper we describe a method for emulating the contrast changes of defocusing brightfield microscopy by using mathematical morphology operators on a single, in-focus PC image. This produces an image in which cells are brighter than the background and thus may be segmented using a single threshold. We then perform k-means clustering on the segmented regions to identify and remove regions that do not correspond with cells and provide an accurate value for the number of cells in an image from which the total number of cells is extrapolated. This technique was applied to generate growth curves for H400 oral keratinocyte cultures supplemented with different concentrations of foetal calf serum.

## 2 Image analysis

### 2.1 Segmenting cells

When a mean filter is applied to a PC image using a circular kernel with radius,  $r_k$ , smaller than that of a cell, cells retain bright edges from the halo and a relatively dark centre (Figure 1b), analogous to the contrast observed by Dehlinger *et al.* when the imaging plane was focused below the focal plane. Conversely, when  $r_k$  is larger than the average cell, cell centres become brighter than the margins (Figure 1c). Imposing a minimum pixel intensity of 0 and subtracting the small kernel image from the large kernel image generates an image in which cell containing regions are brightest (Figure 1d), and to which a single threshold may be applied using the Otsu method to locate cells (Figure 1e) [8].

For the purpose of selecting appropriate  $r_k$  values, a ground truth dataset was obtained by manually counting the cells in 10 images representing a range of cell densities. The

segmentation method described was applied using a range of radii for both large and small kernels to find the combination that minimised differences between this and the manual counts for all ground truth images.

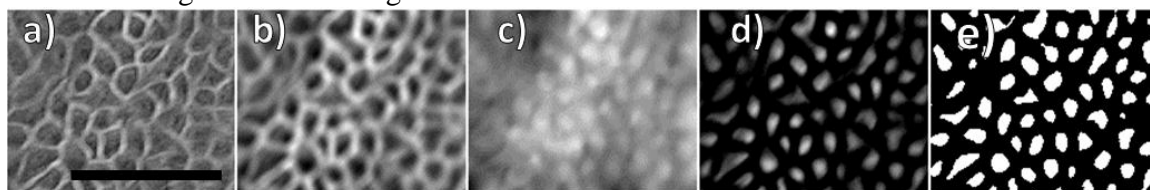


Figure 1: a) - Raw phase contrast image of H400 cells. b) - Image a) filtered with a small kernel mean filter, retaining bright cell margins and darker centres. c) - Original image a) filtered with a large kernel mean filter. Cell-containing regions are brighter than the surrounding regions. d) - Image b) subtracted from image c). Cell containing regions now appear brightest and Otsu thresholding is applied to obtain e). The contrast has been enhanced in all images for improved reproduction. Scale bar in a) is 150 $\mu$ m.

## 2.2 Classifying segmented regions

The cell count of an image is given by the total number of segmented objects in it. Image noise and edge effects at low cell densities can cause incorrectly segmented regions, which contribute erroneously to the cell count and must therefore be discounted. To this end, a dataset of 32 geometrical features describing the morphology and the greyscale properties of the corresponding pixels in the original image were calculated for each region using the “Particles8” plugin for ImageJ [9]. This feature dataset was subsequently reduced to 4 features by performing principal component analysis (PCA) on all segmented regions in all images acquired from a culture over the course of the experiment. K-means clustering ( $k=2$ ) was applied using these 4 features to classify each segmented region as either “true” (real cell) or “false” (incorrect segmentation), and only “true” cells were counted.

## 2.3 Extrapolation of total cell count

The average count from a number of images was used to extrapolate the total number of cells in order to account for density differences across the culture; we used 20 images acquired at random locations in the culture. The fraction of the total culture area represented by one image was used to extrapolate total number of cells in the culture.

# 3 Experimental materials and methods

## 3.1 Cell cultures

Immortalised H400 keratinocytes derived from a human oral squamous carcinoma [10] were maintained at 37°C in a humidified atmosphere with 5% CO<sub>2</sub> in Dulbecco’s MEM / nutrient mix supplemented with 10% foetal calf serum (FCS) (Biosera, UK), 0.6  $\mu$ g/mL L-glutamine (Sigma, UK) and 0.4 mg/mL hydrocortisone (Sigma, UK).

For experimental analysis 3.6 $\times 10^4$  cells, as determined using a haemocytometer, were initially seeded into 35 mm culture dishes (Sarstedt, UK). To reduce the likelihood of non-uniform cell adhesion across the vessel due to uneven temperature distributions, culture dishes were preheated to 37°C prior to seeding and gently agitated following seeding. Duplicate cultures were supplemented with 2%, 6% and 10% FCS for analysis.

To enable comparison between cell counts obtained using the two approaches, additional cultures established under the same conditions were imaged and subsequently counted using an Improved Neubauer haemocytometer (as described below).

### 3.2 Image acquisition and analysis

A Nikon TE300 PC microscope with a x10 objective and a Nikon D40 digital camera (Nikon, UK) were used to acquire images at 2000 x 3008 pixels. Conversion from pixels to mm was obtained via calibration with an image of a microscope stage micrometer giving an image size of 1.17 x 0.78 mm. Images were acquired between 48 - 120 hours post-seeding. The optimal kernel radii for this experimental set-up were determined to be 80 pixels (31  $\mu\text{m}$ ) and 14 pixels (5  $\mu\text{m}$ ). Cell segmentation and classification steps were implemented in ImageJ and included the use of freely available ‘‘Morphological\_PCA’’ and ‘‘Morphological\_Clustering’’ macros [9][11]. Computation time on a set of 280 images was 10 minutes using an Intel® Core™ i7-3770 processor. The kernel radius selection method was implemented using Matlab version R2013a [12].

### 3.3 Cell enumeration using haemocytometer method

Immediately following imaging, the media was aspirated from the culture vessel and replaced with 1 mL trypsin, and incubated until cells were detached. For ease and accuracy of counting at high cell numbers, the cell suspension was diluted appropriately with culture media. Cell concentration was measured using an Improved Neubauer haemocytometer by counting the number of cells in each of the nine 1 mm<sup>2</sup> squares (representing a volume of 0.1  $\mu\text{L}$  each) for each of the two haemocytometer chambers and averaging to provide the number of cells per 0.1  $\mu\text{L}$ . To extrapolate the total number of cells in the culture this value was multiplied by 10<sup>4</sup> and the dilution factor dependent upon the amount of media added.

### 3.4 Assessing classification success

The success of k-means classification was assessed by comparison with 20 images across all samples in which all segmentations had been labelled manually. For this comparison, true positive (TP) describes segmented cells correctly identified by the clustering method described, and true negative (TN) describes erroneous segmentations correctly classified as such. False positive (FP) describes artefacts wrongly classified as cells and false negative (FN) describes cells classified as artefacts. The F<sub>1</sub>-score is a combined measure of precision and recall, for which 0 indicates no agreement between manual and k-means classifications and 1 indicates perfect agreement. It is calculated as:

$$F_1 = 2 \left( \frac{pr}{p+r} \right) \quad (1)$$

where  $p = \frac{TP}{TP+FP}$  is precision and  $r = \frac{TP}{TP+FN}$  is recall. The number of cells undetected in the segmentation step was also recorded for these 20 images.

## 4 Results

The average F<sub>1</sub>-score of segmentation classification using k-means clustering was 0.94  $\pm$  0.04 versus 0.86  $\pm$  0.06 without classification. Average precision was 0.92  $\pm$  0.06 and average recall was 0.96  $\pm$  0.03.

Figure 2a shows growth curves obtained using the method described, which indicate that H400 keratinocytes proliferate in a dose dependent manner with FCS concentration.

Figure 2b shows the growth curves obtained from a set of cultures using the image analysis method described here and the more routinely used haemocytometer method. The image analysis method was systematically lower than the haemocytometer-measured count, although within one standard deviation. The high  $F_1$ -score indicated that this discrepancy was not likely due to errors in cell classification. On average,  $3.8 \pm 1.4\%$  of cells per image were undetected in the segmentation step, but this does not fully account for the difference in counts between techniques, which is  $22 \pm 5\%$ . The systematic operator error associated with haemocytometer counting could potentially have contributed to the discrepancy. Further work is required to determine the source of this difference.

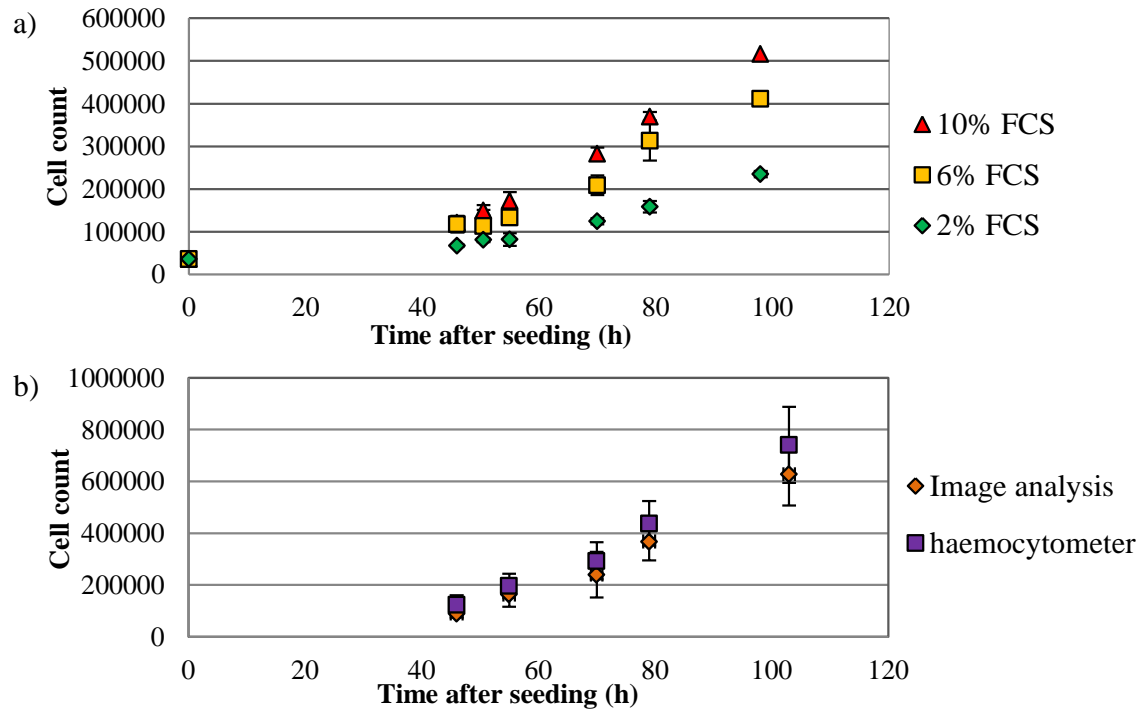


Figure 2: a) Growth curves for H400 keratinocyte cultures supplemented with different concentrations (2-10%) of FCS calculated using the method described. Growth rates were dose-dependently associated with FCS supplementation. Error bars indicate standard deviation between the average cell counts of two cultures under the same culture conditions. b) H400 keratinocyte growth curve determined using two enumeration methods. Each time point corresponds with a single culture from which the total number of cells was determined initially using the image analysis method described and subsequently using the haemocytometer approach. Error bars indicate  $\pm 1$  standard deviation of the mean.

## 5 Discussion and conclusion

The most significant advantage of the method described compared with other commonly used cell counting approaches is that it is non-destructive and thus cultures may be counted multiple times. Aside from minimising human errors associated with the haemocytometer method and reducing the time and cost of maintaining many cultures to generate a growth curve, this image analysis method also introduces the opportunity for the study of the spatial distribution of cells under different culture conditions.

Image filtering has been used previously to locate cells in monolayers, for example, Sarsby *et al.* used a difference of Gaussians filter in their scratch wound analysis

algorithm[6]. A key difference in our approach is the parameterisation method, which prioritises a single region being segmented per cell, to reduce the likelihood of cells merging in the segmented image; essential given our aim of accurate cell counting. By using classification with the unsupervised k-means clustering technique, incorrect segmentations were accurately identified and removed without requiring the use of time-consuming manual training sets. However, it may be possible to further improve accuracy using supervised classification techniques and this will be investigated in further work.

We have shown that our method may be used to distinguish between the growth profiles of keratinocyte monolayers established in different culture conditions. The cell counts obtained by this method are within one standard deviation of that obtained from the same culture using a haemocytometer, although systematically lower. Further work is required to determine the source of this difference.

## Acknowledgements

The authors thank Ela Claridge for useful initial discussions and the EPSRC for funding through a studentship to RF in the PSIBS Doctoral Training Centre (EP/F50053X/1).

## References

- [1] P. Martin, “Wound Healing--Aiming for Perfect Skin Regeneration,” *Science*, 276(5309):75–81, 1997.
- [2] R. Biggs and R. L. Macmillan, “The error of the red cell count,” *Journal of clinical pathology*, 1(5):288–291, 1948.
- [3] N. Jaccard, L. D. Griffin, A. Keser, R. J. Macown, A. Super, F. S. Veraitch, and N. Szita, “Automated method for the rapid and precise estimation of adherent cell culture characteristics from phase contrast microscopy images.,” *Biotechnology and bioengineering*, 111(3):504–517, 2013
- [4] I. Seroussi, D. Veikherman, N. Ofer, S. Yehudai-Resheff, and K. Keren, “Segmentation and tracking of live cells in phase-contrast images using directional gradient vector flow for snakes.,” *Journal of microscopy*, 247(2):137–146, 2012.
- [5] Z. Yin, T. Kanade, and M. Chen, “Understanding the phase contrast optics to restore artifact-free microscopy images for segmentation.,” *Medical Image Analysis*, 16(5):1047–1062, 2012.
- [6] J. Sarsby, E. Claridge, G. Nash, D. Thickett, H. Jeffery, and S. Zheng, “Restoration of phase contrast microscopy images for the analysis of lung epithelial scratch wound repair assays,” in *MIUA 2012*, 101–106.
- [7] D. Dehlinger, L. Suer, M. Elsheikh, J. Peña, and P. Naraghi-Arani, “Dye free automated cell counting and analysis.,” *Biotechnology and bioengineering*, 110(3):838–847, 2013.
- [8] N. Otsu, “A Threshold Selection Method from Gray-Level Histograms,” *IEEE Transactions on Systems, Man and cybernetics*, 20(1):62–66, 1979.
- [9] G. Landini, “Advanced shape analysis with ImageJ,” in Proceedings of the Second ImageJ user and developer Conference, 2008, 116–112, <http://www.mecourse.com/landinig/software/software.html>
- [10] S. Prime, S. Nixon, and I. Crane, “The behaviour of human oral squamous cell carcinoma in cell culture,” *The Journal of Pathology*, 160(3): 259–269, 1990.
- [11] W. S. Rasband, “ImageJ.” U. S. National Institutes of Health, Maryland, USA., 1997-2014. <http://imagej.nih.gov/ij/>
- [12] The MathWorks Inc., “Matlab.” Natick, MA.